FREQUENCY-DOMAIN ANALYSIS OF DIFFUSION-COOLED HOT-ELECTRON BOLOMETER MIXERS

A. Skalare, W.R. McGrath, B. Bumble, H.G. LeDuc
Center for Space Microelectronics Technology,
Jet Propulsion Laboratory, California Institute of Technology,
Pasadena, CA 91109

Abstract

A new theoretical model is introduced to describe heterodyne mixer conversion efficiency and noise (from thermal fluctuation effects) in diffusion-cooled superconducting hot-electron bolometers. The model takes into account the non-uniform internal electron temperature distribution generated by Wiedemann-Franz heat conduction, and accepts for input an arbitrary (analytical or experimental) superconducting resistance-versus-temperature curve. A non-linear large-signal solution is solved iteratively to calculate the temperature distribution, and a linear frequency-domain small-signal formulation is used to calculate conversion efficiency and noise. In the small-signal solution the device is discretized into segments, and matrix algebra is used to relate the heating modulation in the segments to temperature and resistance modulations. Matrix expressions are derived that allow single-sideband mixer conversion efficiency and coupled noise power to be directly calculated. The model accounts for self-heating and electrothermal feedback from the surrounding bias circuit.

1. Introduction

In the last few years, the superconducting hot-electron bolometer (HEB) has attracted much interest for use as the mixing element in low-noise submillimeter wave spectrometer front-ends for astrophysics. Instruments are now being developed for such missions as the National Aeronautics and Space Administration's airborne SOFIA platform, and the European Space Agency's spaceborne FIRST telescope. One of the key properties that make HEB mixers interesting is their ability to operate significantly above the superconducting gap frequency, which is a materials-related parameter that currently limits competing SIS mixers to frequencies below about 1200 GHz. Even though this is a new heterodyne detector that with one exception [1] has not been used for practical astrophysical observations (primarily because frequencies above 1 THz cannot be observed from ground-based observatories), rapid improvements in measured receiver noise temperatures [2-6], and intermediate frequency (if) bandwidths [6,7], have been reported, primarily in anticipation of upcoming missions such as those mentioned above. Despite these recent encouraging results, further improvements in the noise, and indeed the overall optimization of this mixer, will require an accurate and detailed theoretical model which accounts for the unique operation of this device.

Superconducting HEB mixers have mostly been analyzed using lumped element models that were originally developed for semiconductor bolometers [8-12]. In this approach the bolometer is represented as a single (i.e. "lumped") heat capacitance that is connected to a thermal bath via a heat conductance. While this theoretical model has significant merit, especially for phonon-cooled devices that have a uniform electron temperature [13], it does

not accurately take into account the non-uniform temperature distribution in the diffusion-cooled case [14]. The most obvious complication lies in how to determine an appropriate value for the resistive transition dR/dT, which enters as a square in the lumped-element expression for the mixer conversion efficiency. Inclusion of a non-uniform temperature complicates the model enough, that a closed-form analytic solution for mixer conversion and noise cannot be found. Several methods to avoid this problem have been previously investigated. In one approach, a reduced or "effective" value for dR/dT is calculated numerically taking a non-uniform temperature into account, and this value is then used in the regular lumped-element mixer model [15]. Another solution is the so-called "hot-spot" model, where the device resistance-versus-temperature (RT-) curve is approximated by a step function [16-17]. A third method (previously employed by us) is to discretize the bolometer into segments, and do a brute-force numerical time-domain mixing simulation, calculating heat dissipation and heat flow between the segments within each time step. Results of this method are compared to experiments in [18]. The new frequency-domain method described in this paper has advantages compared to all of these previous efforts: 1) It allows mixer conversion efficiency and output noise to be calculated without making simplifications in the RT-curve; 2) The mixer performance can be determined by straightforward matrix multiplications and inversions, without any equivalent of the time-step dependent instabilities that can occur in time-domain simulations; 3) The dominant noise mechanism is included in the model; and 4) Self-heating and electrothermal feedback are fully included. There are also some issues not currently addressed this new technique. For example, it does not include a method for calculating rf or if saturation effects, and it does not include several effects that are particular to superconductors, such as the coherence length and the differences in heat conductance between superconductors and normal metals. Future inclusion of these effects would affect the first, non-linear, part of the theory. The small-signal part of the theory uses parameters calculated from the non-linear part, but may otherwise remain unaffected.

2 The Mixer Model

The type of HEB device we are modeling consists of a submicron-length strip (microbridge) of a superconductor between two normal metal leads. The pads are assumed to be at a bath temperature T_{amb}. Heat dissipation in the microbridge raises the temperature of the center of the device relative to the ends, creating a non-uniform temperature profile. The bridge length L is assumed short enough that the dominant heat conduction out of the bridge is by diffusion of hot electrons to the cold normal metal pads, rather than by electron-phonon interaction.

2.1 Steady State / Large Signal Model

The large-signal temperature distribution in a diffusion-cooled HEB mixer is a result of the *rf* heating caused by the local oscillator, by the heating from the mixer *dc* bias current, and by internal heat conduction. The heat conduction is assumed to be proportional to the local temperature according to the Wiedemann-Franz law:

$$\Phi = -G_0 \frac{T}{T_0} \nabla T \qquad \text{(Eq.1)}$$

where Φ is heat flow intensity, T is the local temperature, and G_0 is the heat conductivity at a reference temperature T_0. The relation leads to the following one-dimensional integral

equation, where the heat flow towards the ends of the bolometer at a particular distance x from the center is equated to the amount of power dissipated inside of that distance:

$$-\frac{1}{2}\frac{G_0}{T_0}\frac{d\left(T^2\right)}{dx}=\frac{P_{rf}}{w\cdot h\cdot L}x+\frac{I_0^2}{w^2h^2}\int_0^x\rho(x',T(x'))dx' \qquad \text{(Eq.2)}$$

where w,h,L are the width,thickness and length of the bolometer, P_{rf} is the amount of local oscillator power dissipated in the bridge, I_0 is the dc current, and ρ is the local resistivity in the bolometer. Since the device film resistivity is usually a non-linear function of temperature and location, no general closed-form solution can be found to this equation. However, a numerical solution can quite easily be found through a corresponding finite-difference formulation:

$$-\frac{1}{2}\frac{G_0}{T_0}\frac{T_k^2-T_{k-1}^2}{\Delta x}=\frac{P_{rf}}{w\cdot h\cdot L}\cdot\Delta x\cdot(k-1)+\frac{I_0^2}{w^2h^2}\cdot\Delta x\cdot S_k \qquad \text{(Eq.3)}$$

where the integral in the previous expression is approximated by a summation $\Delta x\cdot S_k$, with

$$S_1=0\ ;\ S_2=\rho_1\ ;\ S_k=\frac{1}{2}\rho_1+\sum_{l=2}^{k-1}\rho_l+\frac{1}{2}\rho_{k-1}\ ,\ k=3,4,..,N \qquad \text{(Eq.4)}$$

The finite-difference formulation can be seen as a sub-division of the bolometer into N segments, each with its own temperature T_k, as is illustrated in Fig.1 . Only half of the bolometer needs actually be considered because of symmetry. The finite-difference formulation is computationally fast even when used iteratively to find numerical values of various parameters such as the *dc* current I_0 or the temperature T_1 of the device center segment.

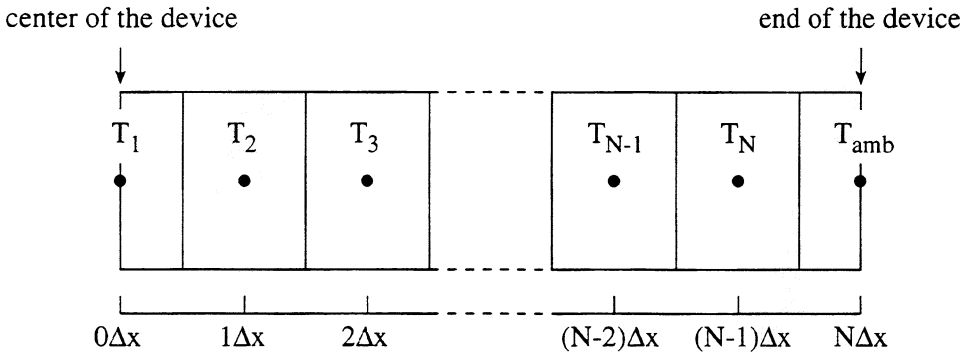

Fig.1; Discretization used in the large- and small-signal models. Because of symmetry only half of the bolometer is analyzed. Therefore the total length of the device is $L=2\cdot N\cdot\Delta x$.

2.2 The Mixer Embedding Circuit

As shown in Fig.2, the discretized bolometer is connected to a Norton equivalent circuit to represent the *dc* bias and intermediate frequency *if* embedding circuits of the mixer. R_0

and I_0 are the steady-state (large signal) resistance and bias current of the device, while ΔR and ΔI are the small-signal modulations representing the modulation of the dissipated *rf* power caused by the combined signal and LO.

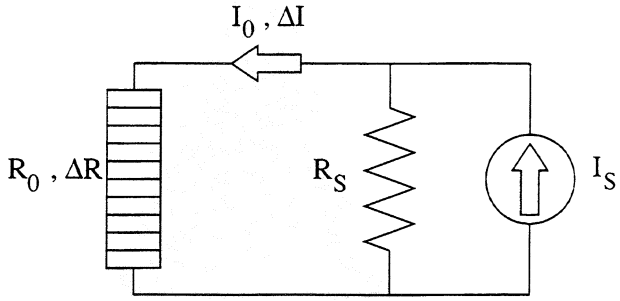

Fig.2; A Norton equivalent circuit is used to represent the dc bias and intermediate frequency circuits.

In the small-signal limit the embedding circuit imposes the following relationship between resistance and current, which must be included in the subsequent mixer theory:

$$\Delta I = -\frac{I_0}{R_0 + R_S}\Delta R \qquad \text{(Eq.5)}$$

, where

$$I_0 = \frac{I_S R_S}{R_0 + R_S} \qquad \text{(Eq.6)}$$

2.3 Mixer Conversion Efficiency Model

In bolometric mixing, the device resistance is varied by the modulation in *rf* power dissipation that is caused by the beating between signal and local oscillator (LO). This modulation in resistance is then detected by an external circuit. In superconducting HEB mixers that are used at frequencies above the superconducting gap frequency, the *rf* heating can be regarded as uniform throughout the device. One can also assume that the signal and local oscillator frequencies are higher than the highest response frequency of the device. In this situation it is convenient to consider the power dissipation from the local oscillator to be constant with time and uniformly distributed throughout the device, and to represent the modulation due to the signal by a uniformly distributed heating function that is modulated at the intermediate frequency, *if*. In the small-signal limit this means that the modulation of the device resistance will occur only at the *if*.

The resistance modulation ΔR is the sum of the modulations ΔR_k in all the segments:

$$\Delta R = \sum_k \Delta R_k = \sum_k \frac{\partial R_k}{\partial T_k}\Delta T_k \qquad \text{(Eq.7)}$$

where ΔT_k is the temperature modulation in segment k. The total heat modulation in segment k is the sum of the contributions from *rf* power dissipation and from the embedding circuit:

$$\Delta P_k = \Delta P_{rf,k} + \Delta P_{emb,k} = \Delta P_{rf,k} + 2R_{0,k} I_0 \Delta I + I_0^2 \Delta R_k \qquad \text{(Eq.8)}$$

The frequency-domain model illustrated in Fig.C is used to calculate the effect that the heating modulations have on the temperatures. In the small-signal limit the thermal model is linear, so heat conductances, heat capacitances and heat sources can be handled by the same complex-notation (i.e. $j\omega$-notation) that is commonly used for small-signal electrical circuits and components. The C_k's in Fig.C are the electronic heat capacitances of the individual segments, which are proprtional to the volume of the segment and to the local temperature T_k. The G_k's are the segment-to-segment heat conductance, which according to the Wiedemann-Franz law is proportional to the electrical conductance and to the local temperature.To handle the many device segments, a matrix notation is introduced (with square brackets denoting matrices and vectors). The relationship between heat dissipation and temperature can be written as an analogue to Ohm's law:

$$[\Delta T_k]_k = [A_{kl}]_{kl} \cdot [\Delta P_l]_l \qquad \text{(Eq.9)}$$

Where $[A]$ is calculated from its inverse, which can be derived according to Fig.3 as :

$$[A^{-1}] = \begin{bmatrix} (j\omega C_1 + G_1) & (-G_1) & 0 & \dots \\ (-G_1) & (j\omega C_2 + G_1 + G_2) & (-G_2) & \dots \\ 0 & (-G_2) & \dots & \dots \\ \dots & \dots & \dots & et\ c. \end{bmatrix} \qquad \text{(Eq.10)}$$

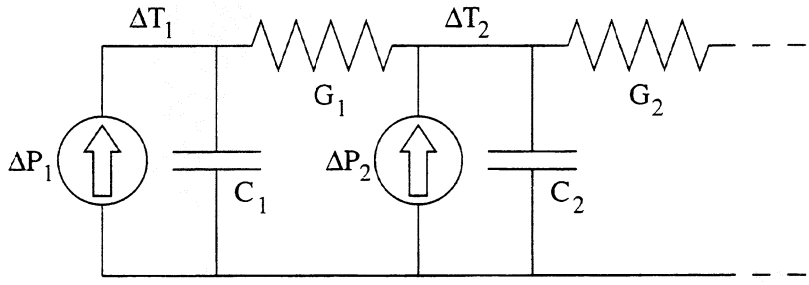

Fig.3; Thermal circuit model, showing heat dissipation sources (ΔP_k), segment heat capacitances (C_k) and segment-to-segment heat conductances (G_k).

The resistance modulation of element k can be written :

$$\Delta R_k = \frac{\partial R_k}{\partial T_k} \Delta T_k = \frac{\partial R_k}{\partial T_k} \sum_l A_{kl} \left(\Delta P_{rf,l} + 2R_{0,l} I_0 \Delta I + I_0^2 \Delta R_l \right) \qquad \text{(Eq.11)}$$

or as the matrix expression (with $\delta_{kl} = 1$ for $k = l$, $\delta_{kl} = 0$ for $k \neq l$.):

$$\left[\Delta R_k\right]_k = \left[B^{-1}\right]_{kl} \cdot \left[\frac{\partial R_l}{\partial T_l} \sum_m A_{lm} \Delta P_{rf,m}\right]_l = \left[B^{-1}\right]_{kl} \cdot \left[\frac{\partial R_l}{\partial T_l} \delta_{lm}\right]_{lm} [A]_{mn} \left[\Delta P_{rf,n}\right]_n \quad \text{(Eq.12)}$$

with:

$$B_{kl} = \delta_{kl} + \frac{\partial R_k}{\partial T_k} \cdot \frac{2I_0^2}{R_0 + R_S} \cdot \left(\sum_m A_{km} R_{0,m}\right) - \frac{\partial R_k}{\partial T_k} I_0^2 A_{kl} \quad \text{(Eq.13)}$$

With the particular discretization illustrated in Fig.1, the heat dissipation in the segments can be written as

$$\Delta P_{rf,1} = \frac{1}{2} \frac{\Delta P_{rf}}{2N} \quad \text{(Eq.14)}$$

$$\Delta P_{rf,k} = \frac{\Delta P_{rf}}{2N} \; ; \quad k = 2,3,...,N \quad \text{(Eq.15)}$$

The matrix expression above provides the connection between the modulation in dissipated *rf* power and the modulation of device resistance. The first of the three terms in the expression for B_{kl} represents the direct response to the *rf* heating. The last term is due to the change in direct ohmic heating when the device resistance changes, while the middle term represents heating due to mismatch between the device and the intermediate frequency load resistor. For convenience, the following response parameter is defined:

$$E = \frac{\Delta R}{\Delta P_{rf}} = \sum_k \Delta R_k \Big/ \sum_k \Delta P_{rf,k} \quad \text{(Eq.16)}$$

In the time domain, the *rf* voltages over the device are

$$V_{LO} \cos \omega_{LO} t + V_S \cos \omega_S t \quad \text{(Eq.17)}$$

and cause a heat modulation at the *if* frequency of:

$$\Delta P_{rf} = \frac{V_{LO} V_S}{R_N} \quad \text{(Eq.18)}$$

The resulting intermediate frequency voltage is:

$$\Delta V = \frac{R_S^2 I_S}{\left(R_0 + R_S\right)^2} \Delta R = \frac{R_S^2 I_S}{\left(R_0 + R_S\right)^2} \cdot E \cdot \frac{V_{LO} V_S}{R_N} \quad \text{(Eq.19)}$$

and, finally, the single-sideband mixer conversion efficiency η can be formulated:

$$\eta = 2 \cdot R_S P_{rf} \left| \frac{I_0 E}{R_0 + R_S} \right|^2 \qquad \text{(Eq.20)}$$

2.4 Thermal Fluctuation Noise

A superconducting bolometer generates both Johnson (or thermal) noise and thermal fluctuation noise. This paper will only treat thermal fluctuation noise in any detail, although a more complete theory should also include Johnson noise. In practice, however, thermal fluctuation noise usually dominates for a diffusion-cooled superconducting *HEB*, when it is operated under the conditions that give minimum receiver noise.

The origin of thermal fluctuation noise is the random exchange of heat carriers between the bolometer and the ambient temperature bath (the normal metal leads), and between different internal parts of the bolometer. In a system in thermal equilibrium with a large reservoir, thermodynamics gives the following well-known expression for the time variance of the energy of that system, where C_V is the heat capacity and k_B is Boltzmann's constant:

$$\left\langle (\Delta E(t))^2 \right\rangle = k_B C_V T^2 \qquad \text{(Eq.21)}$$

In a more relaxed nomenclature this relation can also be expressed as a fluctuation of the system temperature, although this is strictly speaking not correct since temperature is not a fluctuating parameter in a system in equilibrium:

$$\left\langle (\Delta T(t))^2 \right\rangle = k_B T^2 / C_V \qquad \text{(Eq.22)}$$

A real bolometric mixer is per definition *not* in equilibrium with the surrounding medium, since it relies on finite amounts of *dc* and *rf* heat being dissipated inside the device, and of that heat being transported out into the medium. However, if the inelastic electron-electron time is short enough, a local quasi-equilibrium can be established, where any small portion of the device only exchanges heat carriers with the parts of the device that are immediately adjacent to it. The exact conditions under which the expressions above no longer apply are hard to estimate, and in the end a mixer theory for thermal fluctuation noise will need to be compared to experimental results.

For calculating the mixer noise, a circuit model is used, as shown in Fig.4, that is similar to the one used in the conversion efficiency calculation. The heat capacitances and heat conductances are the same as previously discussed, but the heat sources Q_k are arranged differently. The noise heat sources represent exchange of energy between different segments, not dissipation, and are considered incoherent in time (white noise) and uncorrelated with each other. This is a Langevin approach that has similarities to some other formulations found in literature [19]. The method consists of two steps: first the magnitudes of the noise sources are determined, and then the amount of noise power coupled to the output load is calculated.

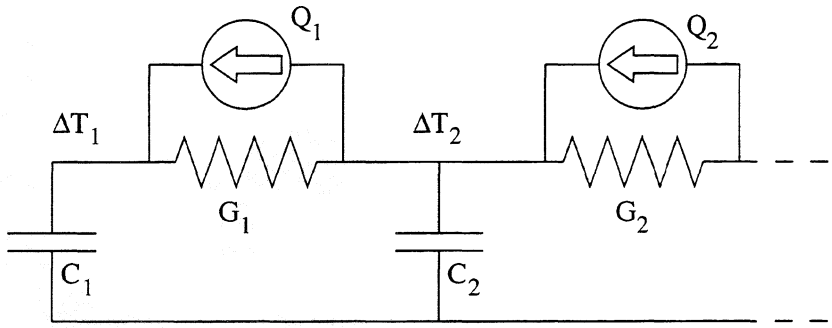

Fig.4; The thermal circuit model used in calculating thermal fluctuation noise.

The expression for the temperature modulation in the segments is (within a small frequency interval *df*):

$$\left[|\Delta T_k|^2 df\right]_k = \left[|F_{km}|^2\right]_{km}\left[|Q_m|^2\right]_m \cdot df \qquad \text{(Eq.23)}$$

, where

$$\left[F_{km}\right]_{km} = \left[A_{kl}\right]_{kl}\left[\delta_{lm} - \delta_{l,m+1}\right]_{lm} \qquad \text{(Eq.24)}$$

The following formula is then used to calculate the source intensities, where the first equality follows from the Wiener-Khinchine theorem and the second one from thermodynamics:

$$\int_0^\infty |\Delta T_k(f)|^2 df = \left\langle |\Delta T_k(t)|^2 \right\rangle = \left[k_B T_k^2 / C_k\right]_k \qquad \text{(Eq.25)}$$

Since the sources are time-incoherent it follows, again from the Wiener-Khinchine theorem, that their frequency-domain representation is frequency-independent. The source distribution can therefore be calculated as the solution to the equation system:

$$\int_0^\infty \left[|F_{km}|^2\right]_{km} df \cdot \left[|Q_m|^2\right]_m = \left[k_B T_k^2 / C_k\right]_k \qquad \text{(Eq.26)}$$

With the noise source distribution known, it is relatively straightforward to calculate the effect on the device resistance:

$$|\Delta R|^2 df = \left[|H_k|^2\right]_k^t \cdot \left[|Q_k|^2\right]_k df \qquad \text{(Eq.27)}$$

, where

$$\left[H_p\right]_p^t = [1]_k^t \left[B^{-1}\right]_{kl} \left[\frac{\partial R_l}{\partial T_l}\delta_{lm}\right]_{lm} [A]_{mn} \left[\delta_{np} - \delta_{n,p+1}\right]_{np} \qquad \text{(Eq.28)}$$

The power delivered to the output load in the small frequency interval df becomes:

$$P_{IF}(f)df = \frac{R_S I_0^2}{\left(R_0 + R_S\right)^2} \left[\left|H_k(f)\right|^2\right]_k^t \left[\left|Q_k\right|^2\right]_k df \qquad \text{(Eq.29)}$$

3. Calculation Example

As an example, a calculation of mixer conversion efficiency was made in order to demonstrate some of the features of our model. Although the method allows an actual experimental resistance-versus-temperature curve to be used, for simplicity the idealized curve in Fig.5 which contains features of actual RT curves was chosen for this example. Two superconducting transition temperatures can be seen in the figure (as is the case in measured RT curves), the higher of which occurs in the central main part of the bridge, while the lower one is present near the ends of the bridge. This is a simplified way of including the suppression of the critical temperature from the proximity effect, that occurs in the regions of the bridge that are contacted by the normal metal leads. The device dimensions used in the calculation are similar to those of our actual HEB mixers: Length $162\ nm$, width $150\ nm$, thickness $10\ nm$, and the heat conductivity $G_0 / T_0 = 0.1\ (W/mK^2)$. The device length included the end regions of the device with the suppressed critical temperature ($12\ nm$). The ambient temperature was chosen to be $4.24\ K$.

Fig.6 shows the current-voltage (IV-) curves calculated for the device, with and without local oscillator power. The overall shape is similar to measured curves for our actual devices. At zero *dc* bias voltage, however, the curves become singular, since the model does not include the limitation on the *dc* supercurrent that is present in real superconductors [20]. The mixer conversion efficiency shown in Fig.6 approaches a maximum at the point where the device cannot be biased in a stable way by the embedding circuit. This is also qualitatively consistent with typical experimental results. The circle in the figure marks approximately the best low receiver noise operating point that would be reachable in a real experiment. In addition, a peak in the conversion efficiency can be seen just above a bias voltage of 3 mV. This effect occurs when enough heat is dissipated in the device so that the end regions of the bridge heat up to their local (suppressed) critical temperature. This is sometimes observed as peaks in the coupled output noise in experimental data. Figure 7 shows the calculated conversion effiency and output noise for the device when operated at the bias point marked in Fig.6. As seen, the conversion effiency curve has the expected single-pole shape, in this case with a 3 dB roll-off frequency of 3-4 GHz. The shape of the output noise curve, however, differs from that calculated from previous "lumped-element" theory [21], according to which it should have the same frequency dependence as that of the conversion efficiency. It should be pointed out that if the number of bolometer segments is reduced to one, the two theories become identical. Also, in a more realistic mixer model the Johnson noise should be included, which has not been done here.

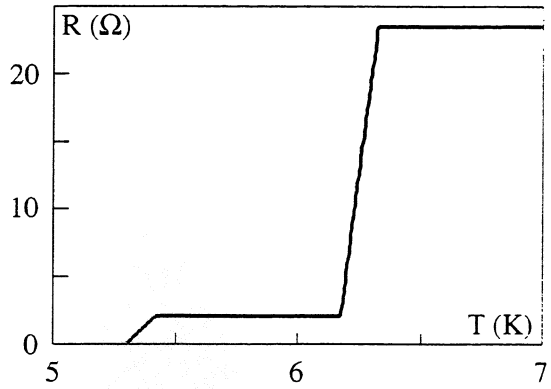

Fig.5; The R-versus-T curve used in the calculation is an idealized curve based on an experimental curve for a niobium HEB.

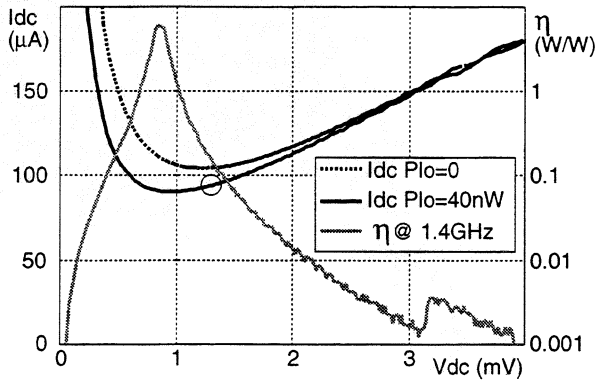

Fig.6; Calculated IV-curves and calculated conversion effiency.

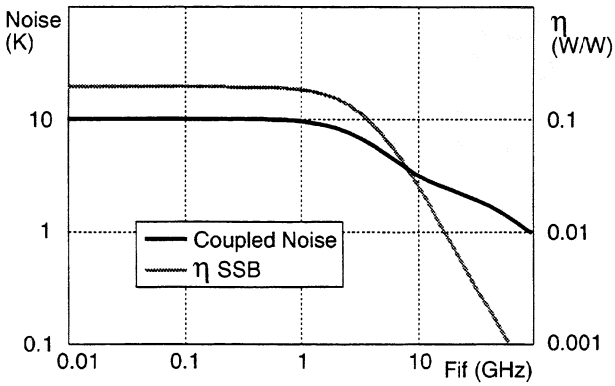

Fig.7; Calculated conversion effiency and coupled output noise as a function of frequency. The noise here is defined as coupled power per Hz to the *if* load resistor, divided by k_B.

Summary

A mixer model for diffusion-cooled hot-electron bolometers has been developed. A non-linear large-signal finite-difference method is used to calculate linearized device parameters, which are subsequently used in small-signal calculations of mixer conversion effiency and noise. The non-uniform temperature distribution inside the bolometer is taken into account both in the large- and small-signal analysis by discretizing the device into a large number of segments, and by assigning a local temperature to each segment. The small signal mixer analysis is done in the frequency domain, using matrix expressions to connect modulations in heating, temperature and resistance. Initial calculations using device parameters that are similar to those of real bolometers give values for conversion and noise that seem reasonable. However, a detailed comparison to experimental data still remains to be done, and will be presented in a future publication. Future work will also include a model for Johnson noise.

Acknowledgments

The research described in this paper was performed by the Center for Space Microelectronics Technology, Jet Propulsion Laboratory, California Institute of Technology, and was sponsored by the National Aeronautics and Space Administration, Office of Space Science.

References

[1] J. Kawamura, R. Blundell, C.-Y.E. Tong, D.C. Papa, T.R. Hunter, G. Gol'tsman, S. Cherednichenko, B. Voronov, E. Gershenzon, "First light with an 800 GHz phonon-cooled HEB mixer receiver", Proc. Ninth Int. Symp. Space Terahertz Tech., 17-19 March 1998, Jet Propulsion Laboratory, Pasadena, CA, pp. 35-43.

[2] B.S. Karasik, M.C. Gaidis, W.R. McGrath, B. Bumble, H.G. LeDuc, "Low noise in a diffusion-cooled hot-electron mixer at 2.5 THz", Appl. Phys. Lett. 71 (11), 15 September 1997, pp. 1567-1569.

[3] P. Yagoubov, M. Kroug, H. Merkel, E. Kollberg, G. Gol'tsman, A. Lipatov, S. Svechnikov, E. Gershenzon, "Quasioptical NbN phonon-cooled hot electron bolometric mixers with low optimal local oscillator power", Proc. Ninth Int. Symp. Space Terahertz Tech., 17-19 March 1998, Jet Propulsion Laboratory, Pasadena, CA, pp. 131-140.

[4] A. Skalare, W.R. McGrath, B. Bumble, H. LeDuc, "Measurements with a diffusion-cooled Nb hot-electron bolometer mixer at 1100 GHz", Proc. Ninth Int. Symp. Space Terahertz Tech., 17-19 March 1998, Jet Propulsion Laboratory, Pasadena, CA, pp. 115-120

[5] B.S. Karasik, A. Skalare, R.A. Wyss, W.R. McGrath, B. Bumble, H.G. LeDuc, J.B. Barner, A.W. Kleinsasser, "Low-noise and wideband hot-electron superconductive mixers for THz frequencies", Proc. Sixth Int. Conf. Terahertz Electronics, 3-4 September 1998, University of Leeds, Leeds, United Kingdom.

[6] R. Wyss et al., these Proceedings

[7] P.J. Burke, R.J. Schoelkopf, D.E. Prober, A. Skalare, W.R. McGrath, B. Bumble, H.G. LeDuc, "Length scaling of bandwidth and noise in hot-electron superconducting mixers", Appl. Phys. Lett. 68 (23), 3 June 1996, pp.3344-3346.

[8] F. Arams, C. Allen, B. Peyton, E. Sard, "Millimeter mixing and detection in bulk InSb", Proc. IEEE, Vol.54, pp.308-318, 1966

[9] J.C. Mather, "Bolometer noise: nonequilibrium theory", Appl. Opt. 21, pp.1125 (1982)

[10] H. Ekström, B.S. Karasik, E.L. Kollberg, K.S. Yngvesson, "Conversion gain and noise of niobium superconducting hot-electron-mixers", IEEE Trans. Microwave Theory Tech., Vol. 43, No.4, April 1995, pp. 938-947

[11] P.J. Burke, "High frequency electron dynamics in thin film superconductors and applications to fast, sensitive THz detectors", Ph.D. dissertation, Yale Univ., New Haven, Connecticut, December 1997.

[12] H.F. Merkel, E.L.Kollberg, K.S.Yngvesson, "A large signal model for phonon-cooled hot-electron bolometric mixers for THz frequency applications,, Proc. Ninth Int. Symp. on Space Terahertz Technology, Jet Propulsion Laboratory, Pasadena, CA, 17-19 March 1998, pp.81-97

[13] E.M. Gershenzon, G.N Gol'tsman, I.G. Gogidze, Y.P. Gusev, A.I. Elant'ev, B.S Karasik, A.D. Semenov, "Millimeter and submillimeter range mixer based on electronic heating of superconducting films in the resistive state", Superconductivity **3** (10), pp. 1582-1597, October 1990.

[14] D. E. Prober, "Superconducting Terahertz Mixer using a Transition-Edge Microbolometer", Appl. Phys. Lett. **62** (17), pp. 2119-2121, (1993).

[15] W.R. McGrath, unpublished

[16] D.W. Floet, J.J.A. Baselmans, J.R. Gao, T.M. Klapwijk, "Resistive behaviour of Nb diffusion-Cooled hot-electron bolometer mixers", Proc. Ninth Int. Symp. on Space Terahertz Technology, Jet Propulsion Laboratory, Pasadena, CA, 17-19 March 1998, pp.63-72

[17] H. Araujo, Presentation at Applied Superconductivity Conference, ASC-98, Palm Desert, California, 1998. To be published in IEEE Trans. Applied Superconductivity.

[18] A. Skalare, W.R. McGrath, B. Bumble, H.G. LeDuc, P.J. Burke, A.A. Verheijen, R.J. Schoelkopf, D.E. Prober, "Large bandwidth and low noise in a diffusion-cooled hot-electron bolometer mixer", Appl. Phys.Lett. 68 (11), 11 March 1996, pp.1558-1560.

[19] R.F. Voss, J. Clarke, "Flicker (1/f) noise : Equilibrium temperature and resistance fluctuations", Phys. Rev. B, Vol.13, No.2, pp.556-573, 15 January 1976.

[20] A.Vl. Gurevich, R.G. Mints, "Self-Heating in Normal Metals and Superconductors", Reviews of Modern Physics, Vol.59, No.4, October 1987

[21] B.S. Karasik, A.I. Elantev, "Analysis of the Noise Performance of a Hot-Electron Superconducting Bolometer Mixer", Proc. Sixth Int. Symp. on Terahertz Technology, pp.229-246, California Inst. of Tech., March 21-23, 1995.